Journal of Engineering Physics and Thermophysics, Vol. 73, No. 6, 2000

SOME ASPECTS OF TREATMENT OF PLASTIC POWDERS BY SKEW SHOCK WAVES

S. K. Andilevko

UDC 534.2

A method for estimating the hydrodynamic parameters of powder and porous materials behind the front of shock waves formed as a result of break decay in emergence of a skew shock wave on the interfaces between these materials or between them and other media is proposed.

Introduction. Despite researchers' efforts (see, for example, [1, 2]), modeling or even approximate description of the behavior of powder materials in dynamic treatment still remains a very complicated problem. This is explained by the fact that these materials are intermediate, in their behavior under dynamic loading, between solids, liquids, and gases. Moreover, quite often they are not only multiphase but also multicomponent. Of course, the problem could be solved by conventional methods if experimentally determined shock adiabats of the type $D(\alpha) = a(\alpha) + b(\alpha)U$, which are capable of accounting for the dependence of the dynamic-loading parameters on the porosity α, were at hand. However, the author has no information about works where such dependences were determined for a fairly large group of materials.

In a series of works [3-8] devoted to investigation of the interaction of plane stationary skew shock waves with each other and with the interface between materials with different acoustic impedance (here, as in [3-8], it is assumed that the material in which the primary skew shock wave (SSW) propagates has a lower acoustic impedance; sometimes, this material will be called the "upper" material, since in all the figures it is pictured at the top) the features of break decays characteristic of materials whose equations of state were assumed to be constant throughout the entire region of investigation were studied. Certain common features of the mechanisms of development of the shock-wave configurations of materials described by different equations of state (polytrope, *D–U* adiabat, and Tate equation) allow the conclusion that the regularities revealed in [3-8] are in principle independent of the concrete form of the equation of state. However, extension of the results of [3-8] to powders and porous materials is significantly impeded by the fact that frequently the equations of state and the shock adiabats of powders and porous materials behind secondary (reflected) shock waves (RflSW) differ significantly from those behind the primary skew shock wave. It should be noted that whereas, for continuous media this situation was the most probable for strong shock waves as a consequence of the processes of heating, ionization, dissociation, etc., for powders this, as a rule, is due to the fact that the total response of the material to the action of a shock wave is determined by the predominant influence of the response of one phase or another. In the case where the porosity of the material is high ($\alpha \to 1$) and, as consequence, the elasticity of the solid phase is insignificant, the response of the gas phase is predominant [9]. However, upon compression under the action of the primary wave, the packing density increases significantly and the reflected shock wave can already propagate over the material, where the main contribution to the response to its action is made by the elasticity of the skeleton formed by the solid phase. This situation can be taken into account in the calculation of shock waves.

Approximate Description of the Parameters of Porous Bodies. Gvozdeva et al. [9] proposed a derivation of the Hugoniot equation corrected for highly porous powder materials ($\alpha \to 1$). Using these results, the parameters of a two-component (solid particles–gas) powder material with a porosity α behind the shock-wave front can be determined as

Scientific-Research Institute of Pulsed Processes of the Belarusian State Scientific and Production Concern of Powder Metallurgy, Minsk, Belarus. Translated from Inzhenerno-Fizicheskii Zhurnal, Vol. 73, No. 6, pp. 1152-1166, November–December, 2000. Original article submitted September 15, 1999.

 1062-0125/00/7306-1118$25.00

$$p_a = \frac{2\alpha_b \rho_b D^2}{k+1} - \frac{k-1}{k+1} p_b, \quad \frac{v_a}{v_b} = \frac{\rho_b}{\rho_a},$$

$$\frac{\rho_a}{\rho_b} = \frac{k-1+(k+1)\dfrac{p_a}{p_b}}{2\alpha_b + k - 1 + (k+1-2\alpha_b)\dfrac{p_a}{p_b}}, \tag{1}$$

$$\alpha_a = 1 - (1-\alpha_b)\frac{\rho_a}{\rho_b}, \quad \rho_l = \alpha_l \rho_g + (1-\alpha_l)\rho_s, \quad l = a, b.$$

Here it is assumed [9] that: 1) the condensed phase can be considered to be incompressible, and the gas in the pores to be perfect; 2) in view of the high heat capacity of the condensed phase, assuming that the rate of hydrodynamic disturbances always exceeds the rate of establishment of thermal equilibrium, the flow arising in such a medium can be considered to be quasi-adiabatic; 3) the elasticity of the solid phase can be neglected in comparison to the elasticity of the gas in the pores, which is quite realistic for highly porous bodies; 4) the filtration of the gas phase through the porous structure is ignored. These conditions significantly restrict the applicability of (1); however, for highly porous materials (HPMs) ($\alpha \to 1$), use of Eqs. (1) is quite justified. The limit of applicability can be determined from system (1). Clearly the maximum of the product $\alpha_b\rho_b$ in the first equation of (1), which prescribes the value of the pressure, is found at the point

$$\alpha_{\min} = \frac{1}{2}\left(1 + \frac{\rho_g}{\rho_s}\right)^{-1}. \tag{2}$$

In the overwhelming majority of cases, $\rho_g << \rho_s$ and $\alpha_{\min} \approx 0.5$. With decrease in α ($\alpha < \alpha_{\min}$), the pressure behind the skew shock wave will decline despite the fact that ρ_b increases. Such behavior is inconsistent with the experimental data of [2], whereas the values of $\alpha_{\min}$ are still significantly distinct from those observed in the case of dense packing of the powder, where the elasticity of the solid-phase "skeleton" should obviously be determining. Thus, the system of equations (1) is conventionally applicable for estimation of the state of a powder in the wake of a shock wave for all $\alpha \geq \alpha_{\min}$. The larger the value of α, the better the approximation obtained. In the subsequent discussion, we will place in the HPM category materials to which (1) can be applied not only in determining the parameters of these materials behind the primary skew shock wave but also in determining their parameters behind the reflected shock wave. This means that even under limiting-compression conditions where

$$\frac{\rho_a}{\rho_b} \approx \frac{k+1}{k+1-2\alpha_b}, \tag{3}$$

the porosity of an HPM in the wake of a skew shock wave should exceed $\alpha_{\min}$, i.e., where

$$\alpha_b \geq \alpha_{vp} \approx \frac{(k+1)\,\alpha_{\min}}{k-1+2\alpha_{\min}}, \tag{4}$$

and since in the majority of cases $\alpha_{\min} \approx 0.5$, then $\alpha_{vp} \approx (k+1)/(2k)$. Classifying porous materials according to their behavior under the action of the secondary shock wave, we can construct the following sequence: 1) HPMs ($\alpha_b \geq \alpha_{vp}$), (1) is fulfilled for both the skew shock wave and the reflected shock wave; 2) medium-porosity materials (MPMs) ($\alpha_{\min} \leq \alpha_b < \alpha_{vp}$), (1) is fulfilled only for the skew shock wave; 3) low-porosity materials (LPMs) ($\alpha_b < \alpha_{\min}$), (1) is applicable for neither the skew shock wave nor the reflected shock wave.

The parameters of an MPM behind the skew shock wave and the parameters of an LPM throughout the entire region of interaction can be estimated with the use of the model of spherical particles developed in [10, 11], where the assumption that the elasticity of the solid-phase "skeleton" of the powder exceeds the elasticity of the gas compressed in the pores is used. Of course, the applicability of this model in the region of $\alpha \sim 0.5$ is highly conventional; however, even at $\alpha \sim 0.3$ the model gives results that agree quite satisfactorily with experiment [11]. Use of this model will make it possible to develop a complete, even if approximate, model for description of the behavior of powder materials under dynamic loading throughout the entire range of change of their porosity in both direct and reflected shock waves. Carroll et al. [10, 11] have established, based on a model of compaction of systems consisting of spherical particles, that for plastic materials with a fairly high porosity β (β, as distinguished from α, was defined in [10-12] as the ratio of the total volume to the volume of the solid phase, $\beta = (1-\alpha)^{-1}$)

$$p(\beta) = \begin{cases} \dfrac{4}{3} G \dfrac{\beta_b - \beta_a}{\beta_a (\beta_a - 1)}, & \beta_b \ge \beta_a \ge \beta_1, \\ \dfrac{2}{3}\left[2G + Y - 2G \dfrac{\beta_b}{\beta_a} + Y \ln\left(\dfrac{2G}{Y} \dfrac{\beta_b - \beta_a}{\beta_a - 1} \right) \right], & \beta_1 > \beta_a \ge \beta_2, \\ \dfrac{2}{3} Y \ln \dfrac{\beta_a}{\beta_a - 1}, & \beta_2 > \beta_a > 1, \end{cases} \tag{5}$$

where

$$\beta_1 = \frac{2G\beta_b + Y}{2G + Y}, \quad \beta_1 = \frac{2G\beta_b}{2G + Y}. \tag{6}$$

Y/G is usually very small ($\sim 10^{-3}$). Omitting the regime of onset of the flow and replacing β by α, we obtain

$$p(\alpha) = \begin{cases} \dfrac{4}{3} G \dfrac{(\alpha_b - \alpha_a)(1 - \alpha_a)}{\alpha_a (1 - \alpha_b)}, & \alpha_{tr} \le \alpha_a \le \alpha_b, \\ \dfrac{2}{3} Y \ln \dfrac{1}{\alpha_a}, & 0 < \alpha_a < \alpha_{tr}, \end{cases} \tag{7}$$

where α_{tr} can be calculated from the relation

$$\frac{(\alpha_b - \alpha_{tr})(1 - \alpha_{tr})}{\alpha_{tr}(1 - \alpha_b)} = \frac{Y}{2G} \ln \frac{1}{\alpha_{tr}}. \tag{8}$$

Figure 1 shows dependences of $\varepsilon = \alpha_b - \alpha_{tr}$ and p_{tr} on α_b, where

$$p_{tr} = \frac{2}{3} Y \ln \frac{1}{\alpha_{tr}}. \tag{9}$$

The quantity ε has third order of smallness in comparison to α_b and α_{tr}. Because of this, the transcendental equality (9) can be transformed to

$$\frac{1}{\alpha_{tr}} - \frac{1}{\alpha_b} = \frac{Y}{2G} \frac{1}{\alpha_b} \ln \frac{1}{\alpha_{tr}}, \tag{10}$$

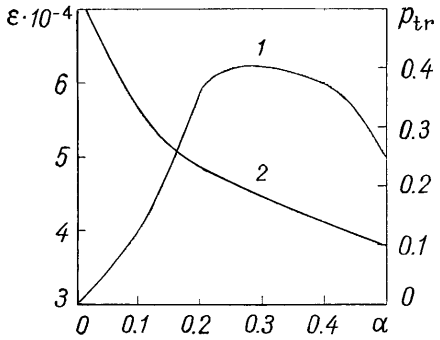

Fig. 1. Dependence of $\varepsilon = \alpha_b - \alpha_{tr}$ (1) and p_{tr} on α_b (2).

and in place of (7) we obtain (here and subsequently the index a on α is omitted)

$$p(\alpha) = \begin{cases} \dfrac{4}{3} G \left(\dfrac{\alpha_b}{\alpha} - 1 \right), & \alpha_{tr} \le \alpha \le \alpha_b, \\ \dfrac{2}{3} Y \ln \dfrac{1}{\alpha}, & 0 < \alpha < \alpha_{tr}. \end{cases} \tag{11}$$

Using (10), (11), the expression for determining the pressure behind the shock-wave front in porous materials [12]

$$p - p_b = \rho_s D^2 \frac{\beta_b - \beta}{\beta_b^2} = \rho_s D^2 (\alpha_b - \alpha) \frac{1 - \alpha_b}{1 - \alpha} \tag{12}$$

and the conservation laws at the shock-wave front, we formulate a system of equations, patterned after (1), for calculating the parameters of the flow behind the shock-wave front:

$$p = p_b + p_s D^2 (\alpha_b - \alpha) \frac{1 - \alpha_b}{1 - \alpha}, \quad \alpha = 1 - (1 - \alpha_b) \frac{\rho}{\rho_b},$$

$$p(\alpha) = \begin{cases} \dfrac{4}{3} G \left(\dfrac{\alpha_b}{\alpha} - 1 \right), & \alpha_{tr} \le \alpha \le \alpha_b, \\ \dfrac{2}{3} Y \ln \dfrac{1}{\alpha}, & 0 < \alpha < \alpha_{tr}, \end{cases} \quad \frac{v}{v_b} = \frac{\rho_b}{\rho}, \tag{13}$$

$$\frac{1}{\alpha_{tr}} - \frac{1}{\alpha_b} = \frac{Y}{3G} \frac{1}{\alpha_b} \ln \frac{1}{\alpha_{tr}}, \quad \rho_b = \alpha_b \rho_g + (1 - \alpha_b) \rho_s.$$

Equations (1) and (13) make it possible to investigate the regularities of the interaction of a skew shock wave with discontinuity surfaces in the presence of powder and porous materials. Using the results of [3-8], we will first find the characteristic angles of interaction, since it is precisely these angles that determine the character of the change in the shock-wave configuration upon variation of the conditions of interaction.

Interaction of a Skew Shock Wave with an HPM. The emergence of a skew shock wave on an interface of the gas–HPM type at a small angle results in a break decay (Fig. 2) responsible for the formation of a refracted shock wave (RfrSW) in the HPM, and in the gas a reflected shock wave begins to propagate from the contact point. This occurs despite the fact that, for high α, the velocity of sound in an HPM

$$c_p = \sqrt{\left(\frac{k p_b}{\alpha_b \rho_b} \right)} \tag{14}$$

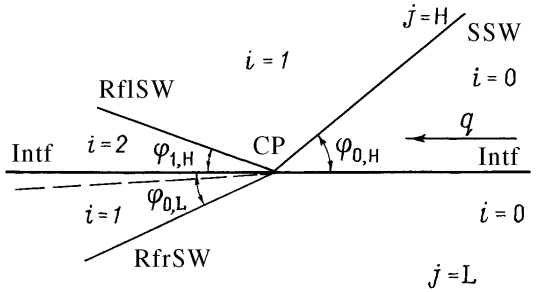

Fig. 2. Scheme of break decay on the interface between materials with a lower and higher acoustic stiffness in a regular interaction regime.

is always smaller than that in a gas. Nevertheless, the density of the HPM is higher than the density of the gas, and the ratio

$$\frac{\rho_b c_\mathrm{p}}{\rho_\mathrm{g} c_\mathrm{g}} = \sqrt{\left(1 + \frac{1-\alpha_b}{\alpha_b}\frac{\rho_\mathrm{s}}{\rho_\mathrm{g}}\right)} \tag{15}$$

always exceeds unity. Using the computational procedure developed in [7, 8] for determining the parameters of a gas in the wake of a skew shock wave (i = 1) and a reflected shock wave (i = 2), we can write the system of Rankine–Hugoniot relations for the upper half-plane (Fig. 2) (j = H)

$$p_{i,j} = \frac{2\rho_{i-1,j} q_{i-1,j}^2}{k+1} \sin^2(\varphi_{i-1,j} + s_i\,\vartheta_{i-1,j}) - \frac{k-1}{k+1} p_{i-1,j},$$

$$\frac{\rho_{i,j}}{\rho_{i-1,j}} = \frac{k-1+(k+1)\dfrac{p_{i,j}}{p_{i-1,j}}}{k+1+(k-1)\dfrac{p_{i,j}}{p_{i-1,j}}} = K_{i,j}, \quad s_i = \begin{cases} 1, & i = 2, \\ 0, & i = 1, \end{cases} \tag{16}$$

$$q_{i,j} = q_{i-1,j} \cos(\varphi_{i-1,j} + s_i\,\vartheta_{i-1,j}) \sqrt{1 + \tan^2(\varphi_{i-1,j} + s_i\,\vartheta_{i-1,j})\,K_{i,j}^{-2}},$$

$$\vartheta_{i,j} = \varphi_{i,j} - \arccos\sqrt{\left(\frac{1}{1+\tan^2(\varphi_{i-1,j} + s_i\,\vartheta_{i-1,j})\,K_{i,j}^{-2}}\right)}.$$

Using (1), we can write an analogous system for the HPM (j = L) (here and subsequently we will assume for definiteness that the free gas of the upper half-plane (see Fig. 2) is identical to the gas filling the pores of the porous materials):

$$p_{i,j} = \frac{2\alpha_{i-1,j}\rho_{i-1,j} q_{i-1,j}^2}{k+1} \sin^2(\varphi_{i-1,j} + s_i\,\vartheta_{i-1,j}) - \frac{k-1}{k+1} p_{i-1,j},$$

$$\frac{\rho_{i,j}}{\rho_{i-1,j}} = \frac{k-1+(k+1)\dfrac{p_{i,j}}{p_{i-1,j}}}{2\alpha_{i-1,j}+k-1+(k+1-2\alpha_{i-1,j})\dfrac{p_{i,j}}{p_{i-1,j}}} = M_{i,j},$$

$$\alpha_{i,j} = 1 - (1-\alpha_{i-1,j})\,M_{i,j}, \quad S_i = \begin{cases} 1, & i = 2, \\ 0, & i = 1, \end{cases} \tag{17}$$

$$q_{i,j} = q_{i-1,j} \cos(\varphi_{i-1,j} + s_i \vartheta_{i-1,j}) \sqrt{1 + \tan^2(\varphi_{i-1,j} + s_i \vartheta_{i-1,j}) M_{i,j}^{-2}},$$

$$\vartheta_{i,j} = \varphi_{i,j} - \arccos \sqrt{\left(\frac{1}{1 + \tan^2(\varphi_{i-1,j} + s_i \vartheta_{i-1,j}) M_{i,j}^{-2}} \right)}.$$

In the case of break decay on an interface of the gas–HPM type, i is always equal to unity for j = L. Clearly $\varphi_{0,H}$ corresponds to the angle of incidence of the skew shock wave, which is denoted by φ in Fig. 2, $p_{0,H} = p_{0,L} = p_0$ (the interface is stationary prior to the emergence of the skew shock wave on it), $q_{0,H} = q_{0,L} = D/\sin\varphi_{0,H} = D/\sin\varphi$, $\rho_{0,H} = \rho_g$, $\rho_{0,L} = \alpha_{0,L}\rho_g + (1 - \alpha_{0,L})\rho_s$, and $\alpha_{0,L}$ is the initial porosity (corresponds to α_b in the previous section). All calculations were performed in a coordinate system tied to the contact point. The complete system obtained after the corresponding changes in j and i (i = 1 and 2 for j = H and i = 1 for j = L) contains 13 equations for determining 15 unknown quantities: $\rho_{1,H}$, $\rho_{2,H}$, $\rho_{1,L}$, $\alpha_{1,L}$, $\vartheta_{1,H}$, $\vartheta_{2,H}$, $\vartheta_{1,L}$, $p_{1,H}$, $p_{2,H}$, $p_{1,L}$, $q_{1,H}$, $q_{2,H}$, $q_{1,L}$, $\varphi_{1,H}$, and $\varphi_{0,L}$. As in the earlier works [3-8], to close it we use the conditions of equality of the pressure and the velocity of the flow normal to the interface behind the contact point

$$p_{2,H} = p_{1,L}, \quad q_{2,H} \sin\vartheta_{2,H} = q_{1,L} \sin\vartheta_{1,L}. \tag{18}$$

The first relation of (18) relates $\varphi_{1,H}$ to $\varphi_{0,L}$:

$$\varphi_{1,H} = \arcsin \sqrt{\left(\frac{\alpha_{0,L}\rho_{0,L} q_{0,L}^2}{\rho_{1,H} q_{1,H}^2} \sin^2\varphi_{0,L} + \frac{k-1}{2} \frac{p_{1,H} - p_0}{\rho_{1,H} q_{1,H}^2} \right)} - \vartheta_{1,H}, \tag{19}$$

and the second relation leads to a transcendental equality in $\varphi_{0,L}$. The system of equations composed in such a way, in which all the indices take all the values inherent in them, will be called the complete system.

The system of equations obtained is similar in principle to the system investigated in [3]. Its numerical solution shows that the development of the shock-wave configuration with change of φ from small values, when the regular regime that is associated with its increase is realized, proceeds in the same way as in [3]. The form of the shock-wave configuration for any arbitrary $0 < \varphi \le \pi/2$ is determined by the characteristic angles φ_{ch} and φ_t, which are respectively the angle of change of the regime of the flow behind the skew shock wave from supersonic to subsonic and the angle of total refraction (when the skew shock wave and the refracted shock wave are equilibrated at the contact point). Methods of calculation of φ_{ch} and φ_t are presented in [3-5]. An expression for φ_{ch} in polytropic gases has been obtained in [3]. This expression remains the same since it is determined by just the "upper" material. In distinction from φ_{ch}, the angle φ_t is a function of the pair of materials forming the interface. Once this angle is attained, a configuration where a plane skew shock wave at the contact point corresponds to just the refracted shock wave while the reflected shock wave is absent is established. We can calculate this angle by forming the complete system for j = H and L and i = 1 with the corresponding conditions

$$p_{1,H} = p_{1,L}, \quad q_{1,H} \sin\vartheta_{1,H} = q_{1,L} \sin\vartheta_{1,L} \tag{20}$$

and with the replacement $\varphi_{0,H} = \varphi_t$. The first equality of (20) will determine the relation between φ_t and $\varphi_{1,H}$

$$\varphi_{0,L} = \arcsin\left(\sin\varphi_t \sqrt{\left(\frac{\rho_{0,H}}{\alpha_{0,L}\rho_{0,L}} \right)} \right), \tag{21}$$

and the second relation will yield a transcendental relation in φ_t. It is apparent from (21) that for an HPM ($\alpha_{0,L} \to 1$) $\varphi_{0,L} << \varphi_t$. Calculations show that φ_t and $\varphi_{0,L}$ are practically independent of D. Figure 3a shows the functions $\varphi_t(\alpha_{0,L})$ and $\varphi_{0,L}(\alpha_{0,L})$ for the systems of air–HPM based on titanium, air–HPM based on iron, and air–PPU-EM-1 open-cellular foamed polyurethane. The same dependences for systems formed by krypton and CO_2 with an HPM based on copper are shown in Fig. 3b.

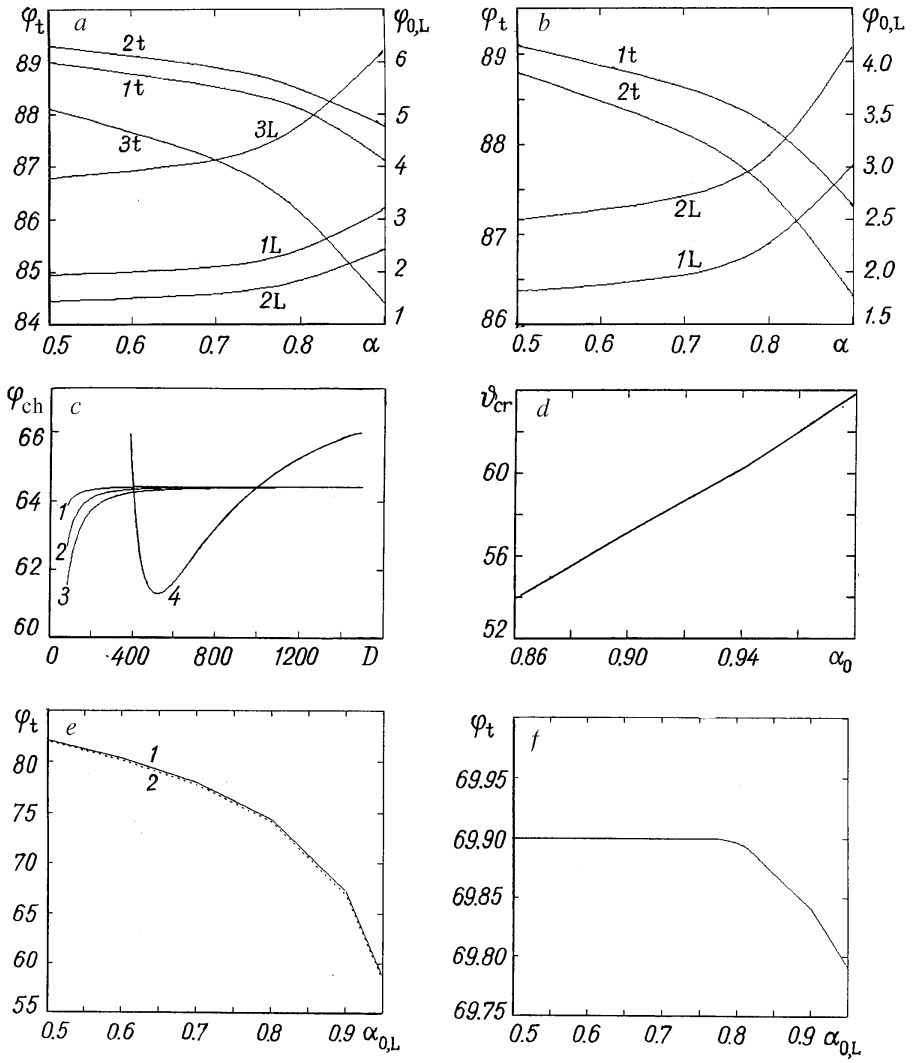

Fig. 3. Dependences: a) $\varphi_t(\alpha_{0,L})$ (t) and $\varphi_{0,L}(\alpha_{0,L})$ (L) for air and an HPM based on titanium (1), iron (2), and foamed polyurethane (3); b) $\varphi_t(\alpha_{0,L})$ (t) and $\varphi_{0,L}(\alpha_{0,L})$ (L) for krypton (1), CO_2 (2), and an HPM based on iron; c) $\varphi_{ch}(D)$ with $\alpha_{0,H} = 0.9$ for an HPM based on copper (1), Al_2O_3 (2), and foamed polyurethane (3) and for air (4); d) $\vartheta_{cr}(\alpha_0)$ for an HPM; e) $\varphi_t(\alpha_{0,L})$ in the case of an interface between HPMs with the same solid phases for copper (1) and foamed polyurethane (2) ($\alpha_{0,H} = 0.98$); f) $\varphi_t(\alpha_{0,L})$ in the case of the interface between an HPM based on foamed polyurethane and an HPM based on copper with the same porosity ($\alpha_{0,H} = \alpha_{0,L}$)

In all the above dependences, $\varphi_t \sim 70^o$, while φ_{ch} falls within 55–67°. This means that for systems of the gas–HPM type, at $\varphi_{ch} \le \varphi \le \varphi_t$ the regular interaction regime changes to a weak irregular shockless regime [3-5] where the curvilinear Mach wave that arises turns the concave face toward the flow. At $\varphi = \varphi_t$, the regime of total refraction is realized. At $\varphi > \varphi_t$, this regime changes to a strong shockless regime [3-5] where the orientation of the Mach wave is reversed. The methods of calculation of these regimes are identical to the methods developed in [3].

Break decay on an interface of the type HPM–continuous medium (solid, liquid) occurs in a significantly different way. Since the velocities of propagation of shock waves in HPMs are very small, a shock wave is practically never formed in a continuous medium, and its surface can be considered to be a rigid surface where break decay is described by different weak (according to the classification in [3-5], when the Mach

wave turns the concave face toward the incoming flow) reflection regimes ($\varphi_t \equiv \pi/2$). In the region of small angles a regular reflection that can be described in sufficient detail using system (17) with j = H and i = 1, 2 can occur. This makes it possible to obtain 10 equations for calculating 11 unknowns: $\rho_{1,H}$, $\rho_{2,H}$, $p_{1,H}$, $p_{2,H}$, $q_{1,H}$, $q_{2,H}$, $\vartheta_{1,H}$, $\vartheta_{2,H}$, $\alpha_{1,H}$, $\alpha_{2,H}$, and $\varphi_{1,H}$. The system is closed by the condition $\vartheta_{2,H} = 0$ [4] since the flow behind the contact point should be parallel to the rigid surface. The change of the reflection regime with increase in φ will be prescribed by φ_{ch} and ϑ_{cr}. For an HPM, the angle φ_{ch} is determined from the inequality

$$\frac{q_{1,H}^2}{\dfrac{kp_{1,H}}{\alpha_{1,H}\rho_{1,H}}} \le 1 \tag{22}$$

as the smallest angle at which the flow behind the skew shock wave becomes subsonic:

$$\varphi_{ch} = \operatorname{arccot} \sqrt{\left(\frac{2kM_{1,H}^{-1}}{k+1} - \frac{k-1}{k+1} kM_{1,H}^{-1} \frac{p_0}{\alpha_{0,H}\rho_{0,H}D^2} - M_{1,H}^{-2} \right)}. \tag{23}$$

The dependence $\varphi_{ch}(D)$ for HPMs based on copper, iron, and foamed polyurethane in air is shown in Fig. 3c. In the same figure, the dependence $\varphi_{ch}(D)$ for air is shown for comparison. The angle ϑ_{cr} determines the change of the regular interaction regime to an irregular one in the case where $\vartheta_{cr} < \varphi_{ch}$. This angle is found as the largest angle φ at which the condition $\vartheta_{2,H} = 0$ can still be fulfilled. In the general case, ϑ_{cr} cannot be calculated analytically. Figure 3d shows results of a numerical calculation of this angle for different α. It was found that the dependence of ϑ_{cr} on D and on the density of the solid phase of the HPM is very slight. The curve in Fig. 3d can be considered to a very good approximation as an integral characteristic of HPMs based on iron, copper, tungsten, Al_2O_3, and foamed polyurethane. When Fig. 3c is compared with Fig. 3d, it is apparent that for the investigated materials $\vartheta_{cr} < \varphi_{ch}$ for any D. Consequently, at $\vartheta_{cr} \le \varphi < \varphi_{ch}$ the regime of regular reflection from a rigid barrier will change to the weak irregular regime described in detail in [4, 5], which in turn will be replaced at $\varphi \ge \varphi_{ch}$ by a weak shockless regime that exists up to $\varphi = \pi/2$. Note that a characteristic of a weak shock regime is the existence of a tangential break that originates at the triple point [4], where the density and the porosity experience an abrupt change that can be very significant (up to 20%). Thus if the loading is performed with the aim of obtaining uniform compaction, it is necessary to avoid this regime, giving preference to the regular regime ($\varphi < \vartheta_{cr}$). Conversely, if there is a need to obtain complex porous structures, a weak irregular shock regime of reflection can be very desirable. In the case of a weak shockless regime, the porosity increases smoothly with distance from the rigid surface, which can also can be claimed in practical applications related to the filtration of liquids and gases.

The most complex pattern of break decay is observed in the case where a skew shock wave emerges on an interface of the type acoustically less rigid (stiff) material – acoustically more rigid material between two HPMs. We consider two actual situations: 1) contact of two HPMs having an identical solid phase, but with $\alpha_{0,H} > \alpha_{0,L}$ (system A); 2) contact of a low-density (for example, foamed polyurethane) and a dense (copper in our case) HPM with $\alpha_{0,H} = \alpha_{0,L}$ (system B). For both cases, at $\varphi < \varphi_{ch}$ and $\varphi < \varphi_t$ regular interaction will occur. The computational procedure for the shock-wave configuration is identical to that used in the calculation of the break decay on an interface of the gas–HPM type, except that for j = H system (17) is used in place of system (16). The conditions along the interface remain the same. The form of expression (21) relating φ_t and $\varphi_{0,L}$ will be somewhat different. For system A

$$\varphi_{0,L} = \arcsin \left(\sin \varphi_t \sqrt{\left(\frac{\alpha_{0,H}}{\alpha_{0,L}} \frac{\rho_{0,H}}{\rho_{0,L}} \right)} \right), \tag{24}$$

and for system B

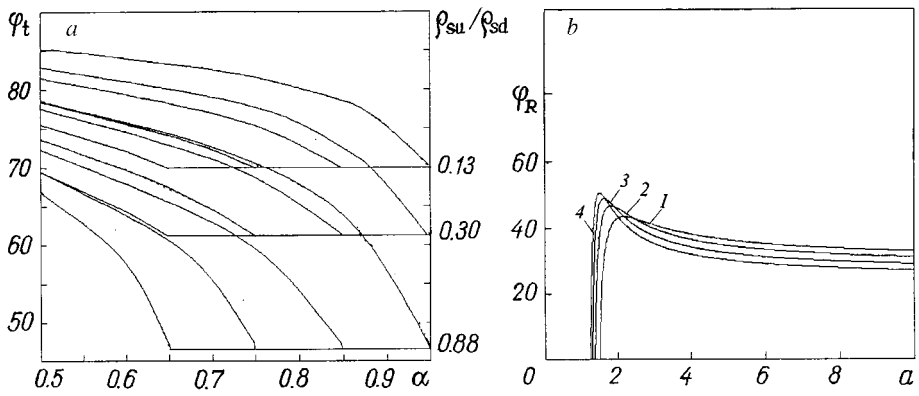

Fig. 4. Dependences: a) $\varphi_t(\alpha_{0,L})$ for different $\alpha_{0,H}$ ($\alpha_{0,H}$ is determined from the value of α at the point of intersection of the curve with the level of the ratio of the densities ρ_{su}/ρ_{sd} of the "upper" and "lower" materials, respectively) for interfaces of the type HPM–HPM and MPM–MPM with different ρ_{su}/ρ_{sd}; b) $\varphi_R(a)$ for α = 0.98 (1), 0.94 (2), 0.90 (3), and 0.86 (4) for different HPMs (gas phase–air).

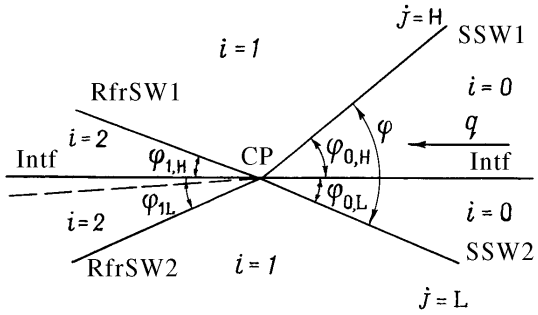

Fig. 5. Scheme of regular interaction of two skew shock waves.

$$\varphi_{0,L} = \arcsin\left(\sin\varphi_t \sqrt{\left(\frac{\rho_{0,H}}{\rho_{0,L}}\right)}\right). \tag{25}$$

All the remaining calculations are not subjected to any serious changes. Calculated values of $\varphi_t(\alpha_{0,L})$ are presented in Fig. 3e. Here φ_t depends insignificantly on D and on the density of the solid phase of the HPM. In the region of values $0.86 \le \alpha \le 1.0$, we have $58^o \le \varphi_t \le 72^o$. For the upper boundary ($\alpha \to 1$) of the "lower" HPM, $\varphi_t < \varphi_{ch}$. In the case of break decay in the above range of values of α, a strong irregular shock interaction is realized for $\varphi_t \le \varphi \le \varphi_{ch}$ [3, 5]. In this case, the Mach wave turns the convex surface toward the incoming flow, and above the interface there is a triple point at which the skew shock wave, the Mach wave, and the reflected shock wave come together. From the triple point a tangential break where the component of the total flow velocity parallel to it and the density (porosity) experience an abrupt change begins. Once $\varphi \ge \varphi_{ch}$, the strong irregular shock regime changes to the strong irregular shockless regime described in detail in [3-5]. Figure 3f shows $\varphi_t(\alpha)$ for system B, where $\alpha_{0,H} = \alpha_{0,L}$ (foamed polyurethane–copper), and the range of change of $\varphi_t(\alpha)$ is very narrow ($69.78^o \le \varphi_t \le 69.90^o$) and hence it can be considered to be constant in practical applications. For a pair of materials that are closer in density (HPM based on iron – HPM based on copper, system B) this angle is constant (in the calculation, a change occurs only in the sixth decimal place) and is equal to 46.8^o. For system A, $\varphi_t > \varphi_{ch}$ and, at all $\varphi \ge \varphi_{ch}$, the regular reflection changes to a weak irregular one that, at $\varphi = \varphi_t$, gives way to total refraction and, at $\varphi > \varphi_t$, to a strong irregular shockless regime [3, 5]. For materials closer in solid-phase density, weak irregular regimes are absent ($\varphi_{ch} > \varphi_t$) and there is a wide range of realization of a strong irregular regime with a reflected shock wave at the triple point and a tangential break ($\varphi_t \le \varphi \le \varphi_{ch}$), which, at $\varphi \ge \varphi_{ch}$, gives way to a strong irregular shockless regime. The fact that φ_t depends essentially on just the difference between the porosities of the HPMs and the ratio between the densities of

their solid phases makes it possible to construct a diagram (Fig. 4a) from which φ_t can be determined to a good approximation for different pairs of materials of the HPM and MPM type (at least when the gas phase is air).

The interaction of two skew shock waves in an HPM (Fig. 5) (the velocity of skew shock wave 1 is D_H and the velocity of skew shock wave 2 is D_L, $D_H \geq D_L$, the interaction parameter is $a = D_H/D_L$) can also be investigated using system (17) on condition that j takes the values j = H, L, M, and N, depending on the shock-wave configuration arising, and i = 1 and 2 for j = H and L if $\varphi_{0,H}$ and $\varphi_{0,L}$ are less than φ_{ch} and i = 1 in all the remaining cases [8].

The angles formed by skew shock wave 1 and skew shock wave 2 with the fictitious interface (Fig. 5) are determined by the relations [8]

$$\varphi_{0,H} = \begin{cases} \arctan \dfrac{a \sin \varphi}{1 + a \cos \varphi}, & \varphi \leq \varphi_T, \\ \pi - \arctan \dfrac{\sin (\pi - \varphi)}{a \cos (\pi - \varphi) - 1}, & \varphi > \varphi_T; \end{cases} \tag{26}$$

$$\varphi_{0,L} = \begin{cases} \arctan \dfrac{\sin \varphi}{a + \cos \varphi}, & \varphi \leq \varphi_T, \\ \arctan \dfrac{\sin (\pi - \varphi)}{a - \cos (\pi - \varphi)}, & \varphi > \varphi_T, \end{cases} \tag{27}$$

$$\varphi = \varphi_{0,H} + \varphi_{0,L}.$$

The angle

$$\varphi_T = \arccos\left(-\frac{1}{a}\right) \tag{28}$$

is a constant of the process. Here, regular interaction with the contact point of four skew shock waves (skew shock wave 1, skew shock wave 2, refracted shock wave 1, refracted shock wave 2), shown schematically in Fig. 5, can also be realized. The limiting angle of realization of this regime φ_R can be found analytically by replicating all the calculations carried out in [7], but now for system (17):

$$\varphi_R = \arcsin\left[\frac{b}{a^2 (1 + b^2)}\left(1 + \sqrt{\left(a^2 - \frac{b^2}{1 + b^2}\right)}\right)\right], \tag{29}$$

where

$$b = \tan (\arcsin \sqrt{g}),$$

$$g = \left(\frac{\varepsilon a^2}{a^2 - 1}\right)^2 (1 - K^2) \frac{K_0}{8}\left\{\sqrt{\left[\left[1 + \left(\frac{a^2 - 1}{\varepsilon a^2}\right)^2\right]\frac{16}{K_0^2 (1 - K^2)^2}\right]} - 1\right\}, \tag{30}$$

$$K = \frac{k - 1}{k + 1} K_0, \quad K_0 = \frac{2k}{k + 1} \frac{p_0}{\rho_{0,H} D_H^2} + 1 - \frac{2a_0}{k + 1}, \quad \varepsilon = \frac{1 - (1 - \alpha_0) K_0^{-1}}{\alpha_0}.$$

As in the case of gases, φ_R depends insignificantly on the properties of the specific filling material of the HPM; the dependence on α is somewhat more marked (Fig. 4b); however, it does not change the general form

of the curve. The angle φ_R becomes zero in the region of small $a \le a_{cr}$ ($a_{cr} \sim 1.19$) and the regime of regular interaction is impossible in this region.

Because of the fundamental similarity of systems (16) and (17), the development of the shock-wave configuration in this case is fully identical to that in gases, described in detail in [8]. We note only that, based on the analysis in [8], an experimenter who wants to obtain the most homogeneous structure of an HPM subjected to shock-wave loading (without sharp changes in the porosity in the process of compaction) must take care that at all points where interaction between skew shock waves is possible the angle $\varphi_{0,L}$ be larger than the angle φ_{ch}. In all remaining cases, the appearance of tangential breaks and, correspondingly, drastic changes in the porosity is very probable.

Interaction of a Skew Shock Wave with an MPM. As has been mentioned above, the parameters of the flow behind the primary skew shock wave in an MPM (j = H, i = 1) are described in the same manner as in the case of an HPM. Because of this, break decay at a gas–MPM interface proceeds quite analogously to the case of an HPM, except that the values of φ_t turn out to be even larger than for an HPM and tend to $\pi/2$ as ρ_s increases and $\alpha_{0,L}$ decreases. Some differences are observed only in the case of break decay on an interface of the type MPM–continuous medium and MPM–MPM. As in the previous case, the interface between an MPM and a liquid or a solid can be interpreted as a rigid surface even for very strong skew shock waves (a consequence of the small velocity of propagation of skew shock waves in powders). The parameters of the flow arising in an MPM in the wake of a skew shock wave are given by system (17) with j = H and i = 1, while to determine these parameters behind the reflected shock wave formed in the case of comparatively small angles of interaction it is necessary to use the system

$$p_{i,j} = p_{i-1,j} + \rho_s (\alpha_{i-1,j} - \alpha_{i,j}) \frac{1-\alpha_{i-1,j}}{1-\alpha_{i,j}} q_{i-1,j}^2 \sin^2 (\varphi_{i-1,j} + s_i \vartheta_{i-1,j}),$$

$$p_{i,j} - p_{i-1,j} = \begin{cases} \frac{4}{3} G \left(\frac{\alpha_{i-1,j}}{\alpha_{i,j}} - 1 \right), & \alpha_{tr} \le \alpha_{i,j} \le \alpha_{i-1,j}, \\ \frac{2}{3} Y \ln \frac{1}{\alpha_{i,j}}, & 0 < \alpha_{i,j} < \alpha_{tr}, \end{cases}$$

$$\frac{1}{\alpha_{tr}} - \frac{1}{\alpha_{i-1,j}} = \frac{Y}{3G} \frac{1}{\alpha_{i-1,j}} \ln \frac{1}{\alpha_{tr}}, \quad \frac{\rho_{i,j}}{\rho_{i-1,j}} = \frac{1-\alpha_{i,j}}{1-\alpha_{i-1,j}},$$

$$q_{i,j} = q_{i-1,j} \cos (\varphi_{i-1,j} + \tag{31}$$

$$+ s_i \vartheta_{i-1,j}) \sqrt{\left(1 + \tan^2 (\varphi_{i-1,j} + s_i \vartheta_{i-1,j}) \left(\frac{1-\alpha_{i-1,j}}{1-\alpha_{i,j}} \right)^2 \right)},$$

$$\vartheta_{i,j} = \varphi_{i-1,j} - \arccos \sqrt{\left(\frac{1}{1 + \tan^2 (\varphi_{i-1,j} + s_i \vartheta_{i-1,j}) \left(\frac{1-\alpha_{i-1,j}}{1-\alpha_{i,j}} \right)^2} \right)}$$

with j = H and i = 2. The complete system involves (17) and (31) with the corresponding i and j and is closed by the condition of parallelism of the flow and the interface in the vicinity of the rigid surface – $\vartheta_{2,H} = 0$. As earlier, the critical angle ϑ_{cr} of regular reflection can be determined as the largest angle φ at which $\vartheta_{2,H} = 0$. Figure 6a shows the function $\vartheta_{cr}(\alpha)$ for an MPM. As in the case of an HPM, it is practically independent of the velocity of the skew shock wave and the parameters of the filling material, although, in (31), not only its density but also the moduli Y and G are already used. At the same time, it is found that the numerical value

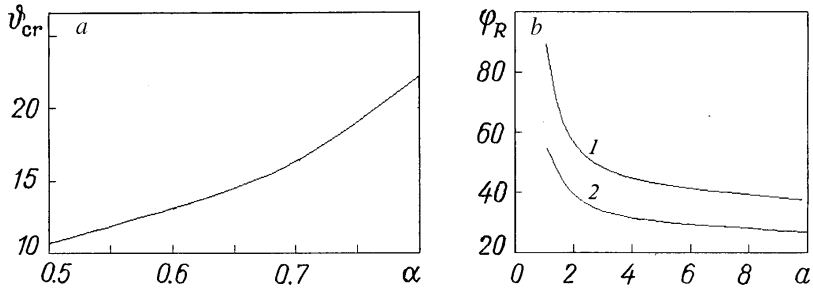

Fig. 6. Characteristic angles for an MPM: a) $\vartheta_{cr}(\alpha)$; b) $\varphi_R(a)$ for $\alpha = 0.8$ (1) and 0.6 (2).

of ϑ_{cr} for an MPM is much lower than that for an HPM and the region of existence of irregular reflection with a reflected shock wave is significantly wider ($20^o < \varphi \le 65^o$).

The emergence of a skew shock wave on an interface of the HPM–MPM type is accompanied by a regular interaction regime for all $\varphi < \varphi_{ch}$ since, in this case, $\varphi_{ch} < \varphi_t$ (see Fig. 4a) practically always. Then, at $\varphi_{ch} \le \varphi < \varphi_t$ the regular interaction changes to a weak shockless regime [3, 4], which at $\varphi = \varphi_t$ changes to a regime of total refraction that changes then ($\varphi > \varphi_t$) to a strong irregular shockless regime. In this case, regions with a tangential break and the porosity difference corresponding to it are practically excluded. For an interface of the MPM–MPM type the relation between the angles φ_{ch} and φ_t is much more complex.

The interaction of shock waves in an MPM in the region of small angles, where a regular interaction regime can supposedly exist, is described by a complete system based on (17) with $i = 1$ and (31) with $i = 2$. The conditions on the interface are the same as in the case of an HPM. The values of the characteristic angles φ_{cr} and φ_T remain constant, only the angle φ_R of the shock-wave configuration is unknown. Unfortunately, as distinguished from the previous case, the limiting value of φ_R cannot be determined analytically. Figure 6b shows values of φ_R calculated for two values of the initial porosity: 0.6 and 0.8. The calculations showed that φ_R depends on just a and α (at least for MPMs based on copper, lead, iron, aluminum, titanium, and tungsten). The general form of the dependence $\varphi_R(a)$ for an MPM differs significantly from that for an HPM (Fig. 6b). Of prime importance is the fact that φ_R increases as $\alpha \to 1$, while in the case of an HPM it becomes zero much more before the parameter a reaches unity. This means that for MPM-type materials the interaction of two identical waves can be accompanied by the appearance of a regular reflection regime.

Interaction of a Skew Shock Wave with an LPM. We will determine the characteristic shock-wave configurations in the case of interaction of a skew shock wave with an LPM, beginning with consideration of an interface of the gas–LPM type. For the half-space L, system (31) (j = L, i = 1) should be used. The gas, as before, is determined by system (16) (j = H, i = 1 and 2). The angle φ_{ch} is a characteristic of the gas and its value remains unchanged (60–65°), while φ_t increases markedly and is practically equal to φ_t for an interface of the gas–solid type ($\varphi_t \to \pi/2$, [4]). This means that the interaction of a skew shock wave with an interface of the gas–LPM type will be accompanied by a regular regime as long as $\varphi < \varphi_{ch}$, which, at $\varphi = \varphi_{ch}$, will change to a weak irregular regime [3-5] that exists up to $\varphi = \varphi_t$. Since the values of φ_t are very close to $\pi/2$, the regime of strong irregular shockless interaction is characteristic of just a very small group of angles close to a right angle, which practically always can be identified with a glancing wave [6].

Even in the case where the porosity of the LPM is very small ($\alpha \sim 0.01$), the velocity of sound in it remains much lower than the velocity of sound in continuous materials [13, 14]. Because of this, an interface of the LPM–solid type can be classified with rigid surfaces. The angle φ_{ch} should be calculated based on the inequality $q_{1,H}/D_{min} \ge 1$. The minimum velocity of propagation of shock waves in an LPM [12] is

$$D_{min} = \sqrt{\left(\frac{2}{3}\frac{Y}{\rho_s \alpha}\right)}, \tag{32}$$

and

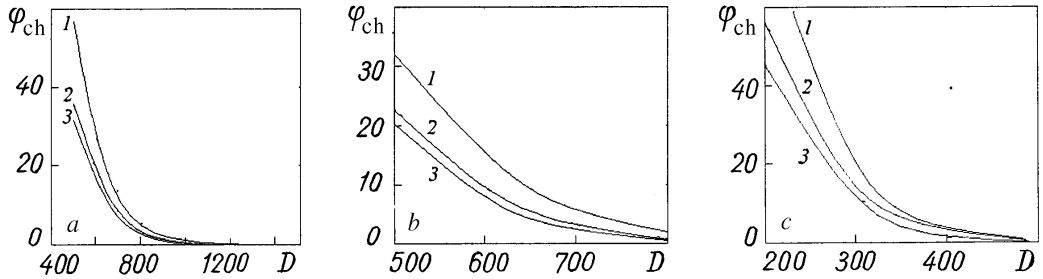

Fig. 7. Angle $\varphi_{ch}(D)$ in an LPM based on copper (a), aluminum (b), and lead (c) for α = 0.3 (1), 0.4 (2), and 0.5 (3).

$$\varphi_{ch} = \operatorname{arcctan} \sqrt{\left(\frac{2Y}{3\rho_s \alpha_{1,H} D^2} - \left(\frac{1-\alpha_{0,H}}{1-\alpha_{1,H}} \right)^2 \right)}, \tag{33}$$

where $\alpha_{1,H}$ is determined from the transcendental relation

$$\frac{2}{3} \frac{Y}{\rho_s D^2} \ln \frac{1}{\alpha_{1,H}} = (\alpha_{0,H} - \alpha_{1,H}) \frac{1-\alpha_{0,H}}{1-\alpha_{1,H}}. \tag{34}$$

The fact that for LPMs, the elasticity of the skeleton makes a determining contribution to the interaction leads to the fact that the minimum velocity of propagation of shock waves increases very rapidly as the voids are filled, which in turn causes a rapid decrease in φ_{ch} (Fig. 7). Even at relatively small values of D the process of closing of pores becomes very marked and rapid, and D_{min} behind the skew-shock-wave front tends asymptotically to the velocity of sound in a continuous material. For LPMs, essentially only at a velocity $D \sim 200$–800 m/sec do there exist any marked regions of realization of the regular-reflection regime that change directly to a weak shockless regime. In all remaining cases, only the shockless regime is essentially realized.

The behavior of $\varphi_{ch}(D)$ has a marked influence on the shape of the shock-wave configuration in the case where a skew shock wave emerges on an interface of the LPM–LPM type. Since φ_t is, as a rule, much larger than φ_{ch}, and φ_{ch} is very small, here, just as in the case of a rigid surface, there exists a narrow zone of realization of a regular regime that changes directly to a weak shockless regime. Tangential breaks are absent, and the density and the porosity change smoothly.

Small values of φ_{ch}, characteristic of LPMs, also leave their mark on the features of the interaction of skew shock waves in this medium, since, in this case, only interaction regimes without reflected shock waves (as, for example, in the case of weak shock waves in gases [8]) can actually be realized. To calculate these regimes, it will suffice to use system of equations (32) with the corresponding [8] changes in i and j.

Conclusion. The classification of porous materials by their behavior under the action of a reflected shock wave with the use of approximate equations of state of porous media, proposed in the present work, makes it possible to estimate the break decay in the case of interaction of skew shock waves with different interfaces (on the one condition that the acoustic impedance of the "lower" material must be higher than that of the "upper" material) and with each other. Such estimates can be widely used to predict the results of experimental and practical works.

In conclusion, the author expresses his gratitude to Academician O. V. Roman and G. S. Romanov for their constant attention to and benevolent attitude toward this work.

NOTATION

D, shock-wave velocity; a, velocity ratio of the interacting skew shock waves; c, velocity of sound in the medium; p, pressure; q, total velocity of the flow in a coordinate system tied to the point of intersection of

the skew shock wave with the surface; k, polytrope index of the gas; ρ, density; α, porosity (the ratio of the volume of the pores to the total volume); β, porosity (the ratio of the total volume to the volume of the solid phase); v, component of the flow velocity q normal to the shock-wave front; G, shear modulus of the solid phase; Y, yield point of the solid phase; φ, angle formed by the corresponding shock wave with the interface; ϑ, angle of rotation of q behind the shock wave and, with the subscript cr, critical angle for the regular regime in the case of break decay on a rigid surface; s, K, M, and K_0, functions and notation defined in the text. Subscripts: H and L, upper and lower half-spaces, respectively; M and N, upper and lower points of the Mach wave, respectively; 0, parameters of the medium before the skew shock wave and the refracted shock wave; 1, parameters of the medium behind the skew shock wave and the refracted shock wave; 2, parameters of the medium behind the reflected shock wave; cr, critical values; tr, transition values; ch, change of the supersonic regime of the flow behind the skew shock wave to a subsonic regime; t, angle of total refraction; T, angle of change of the orientation in the interaction of two skew shock waves; R, limiting angle of the regular regime in the interaction of two skew shock waves; b, before the shock wave; a, after the shock wave; s and g, parameters of the solid and gas phases, respectively; p, powder parameters; vp, lower value of the porosity for an HPM; min, minimum; j takes the values H, L, M, and N; i takes the values 0, 1, and 2; l takes the values a and b; su and sd, densities of the upper and lower components of the system consisting of two media, respectively.

REFERENCES

1. O. V. Roman and V. G. Gorobtsov, in: L. E. Murr (ed.), *Shock Waves for Industrial Applications*, New Jersey, USA (1988), pp. 335-379.
2. V. F. Nesterenko, *Pulsed Loading of Heterogeneous Materials* [in Russian], Novosibirsk (1992).
3. S. K. Andilevko, *Inzh.-Fiz Zh.*, **72**, No. 2, 210-217 (1999).
4. S. K. Andilevko, *Inzh.-Fiz Zh.*, **72**, No. 2, 218-227 (1999).
5. S. K. Andilevko, *Inzh.-Fiz Zh.*, **72**, No. 3, 507-514 (1999).
6. S. K. Andilevko, *Inzh.-Fiz Zh.*, **72**, No. 3, 515-518 (1999).
7. S. K. Andilevko, *Inzh.-Fiz Zh.*, **72**, No. 4, 697-699 (1999).
8. S. K. Andilevko, *Inzh.-Fiz Zh.*, **72**, No. 4, 700-708 (1999).
9. L. G. Gvozdeva and Yu. M. Faresov, *Prikl. Mekh. Tekh. Fiz.*, No. 1, 120-125 (1986).
10. M. M. Carroll and A. C. Holt, *J. Appl. Phys.*, **44**, No. 10, 4388-4392 (1973).
11. B. M. Butcher, M. M. Carroll, and A. C. Holt, *J. Appl. Phys.*, **45**, No. 9, 3864-3875 (1974).
12. S. Z. Dunin and V. V. Surkov, *Prikl. Mekh. Tekh. Fiz.*, No. 1, 131-142 (1982).
13. G. Rudinger, *Raketnaya Tekh. Kosmonavtika*, **3**, No. 7, 27-33 (1965).
14. A. Wood, *Sound Waves and Their Application* [Russian translation], Moscow–Leningrad (1934).